Journal of Engineering Physics and Thermophysics, Vol. 77, No. 3, 2004

INFLUENCE OF FLOW ANGULARITIES IN A HYPERSONIC RAMJET DIFFUSER ON THE FORMATION OF THE SHOCK-WAVE STRUCTURE OF THE REAL GAS FLOW

G. A. Tarnavskii

UDC 518.8:533.6

We have investigated the shock-wave structures arising at the entrance to the engine section of hypersonic aircraft and the influence on the process of their formation of the flow angularity after oblique shock fronts incident inside the diffuser with a different type of interaction (Mach or regular). To take into account the real properties of the atmosphere, we used the effective adiabatic exponent method permitting determination of the topology of shock-wave patterns and calculation of the gas- and thermodynamic parameters in various flow zones between the shock fronts in a wide range of diagnostic variables for the Earth's atmosphere.

Introduction. The main goal of this paper is to investigate such an interaction of shock waves, e.g., in air intakes and nozzles of engines of hypersonic aircraft in certain ranges of flight conditions, where dualism of the solution takes place — the possibility of existence at the same diagnostic variables of the problem of shock-wave patterns of reflection of two different types: regular or Mach reflection (Neumann paradox). The necessity for the hypersonic ramjet engine (HRE) to operate under designed conditions calls for the development of a system for correcting the entrance of the flow into the diffuser. As a rule, such systems are mechanical and are connected with the possibility of varying the entrance angles. The idea of "thermal correction" of the diffuser investigated in [1] also seems to be very promising. It presupposes energy supply to the incoming flow in front of the diffuser. It should be noted, however, that such a correction (along with mechanical correction, though) cannot guarantee the absence of nondesigned regimes in all cases, especially in aircraft maneuvering. One nondesigned regime is the regime of an oblique compression shock incident inside the diffuser and its reflection, which can cause flow separation and the formation of stagnation or recirculation regions of the flow and its considerable nonuniformity and lead to high thermal and power loads. Therefore, investigation of such regimes at various flight altitudes and velocities and prediction of the consequences of their appearance are of great importance.

For high-speed aircraft, the supply of a precompressed oxidizer (air) into the HRE section is actually completely determined by the flight velocity and the diffuser geometry, which should provide, apart from optimum air intake, stability and predictability of functioning. At the entrance to the HRE diffuser, a system of oblique compression shocks determining the structure of the gas flow in the section is realized. The elaboration of methods of mathematical simulation enabled by the high level of modern computer engineering has made it possible to investigate spatial high-enthalpy gas flows with the formation of complex shock-wave structures in the flow. In this case, the study of problems on the nonuniqueness and hysteresis of obtained numerical solutions and analysis of their adequacy to real physical processes becomes important.

The investigations of the regular reflection (RR) and Mach reflection (MR) of shock waves (SW) performed up to the present permit some conclusions about the domains of their existence, including the domains of existence of a dual solution, in which the formation of stable patterns of both RR and MR is possible. Such domains of solution dualism arise in a number of subranges of change in the diagnostic variables of the process — the Mach number of the incoming flow, flow angularity, etc. These two types of shock-wave structures formed by the SW reflection in steady flows are schematically represented in Fig. 1.

The RR pattern (Fig. 1a) formed in the process of inleakage of a supersonic stream with a Mach number M_0 on two wedges characterized by angles β_1 and β_2 includes, respectively, two oblique compression shocks (CS) i_1

Institute of Theoretical and Applied Mechanics, Siberian Branch of the Russian Academy of Sciences, 4/1 Institutskaya Str., Novosibirsk, 630090, Russia; email: tarnav@itam.nsc.ru. Translated from Inzhenerno-Fizicheskii Zhurnal, Vol. 77, No. 3, pp. 155–164, May–June, 2004. Original article submitted November 3, 2003.

1062-0125/04/7703-0651

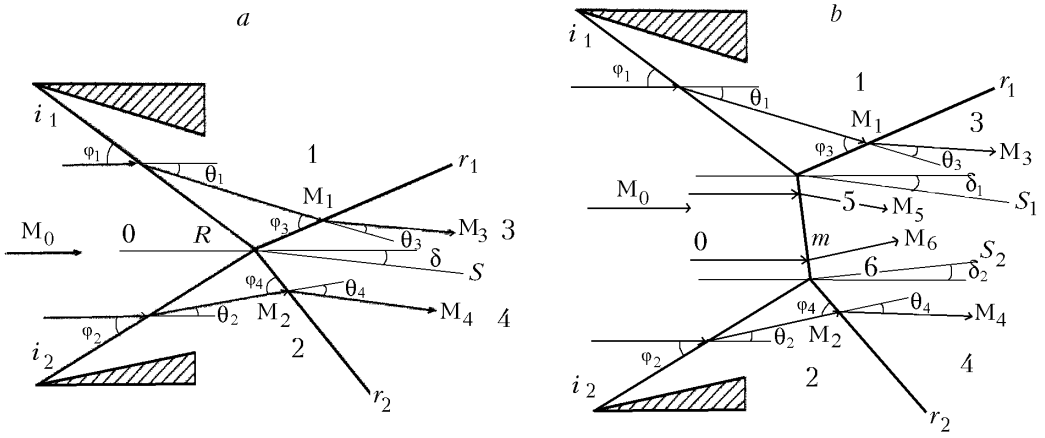

Fig. 1. Patterns of shock-wave structures under interaction of compression shocks: regular (a) and Mach (b) reflection.

and i_2 formed in the vicinity of the surface of the wedges and incident inside the flow region with slope angles φ_1 and φ_2 (hereinafter angles are determined with respect to the direction of the incoming flow) and two reflected CSs r_1 and r_2 with slope angles φ_3 and φ_4. These CSs intersect at point R. The wake S with a slope angle δ is formed when the flow is passing through a system of shocks with flow angularities θ_1, θ_2, θ_3, and θ_4 on shocks i_1, i_2, r_1, and r_2, respectively. For the stationary pattern, the relations

$$\theta_1 = \beta_1, \quad \theta_2 = \beta_2, \quad \theta_1 - \theta_3 = \theta_2 - \theta_4 = \delta$$

hold. For symmetric reflection ($\beta_1 = \beta_2$), naturally, $\delta = 0$.

When a wave structure with MR arises (Fig. 1b), in addition to the incident and reflected CSs i_1, i_2, r_1, and r_2 there appears a central shock m, whose front connects two triple shock intersection points (i_1, r_1, m) and (i_2, r_2, m), and also two wakes S_1 and S_2 with slope angles δ_1 and δ_2 arise. For the stationary pattern, the relations

$$\theta_1 = \beta_1, \quad \theta_2 = \beta_2, \quad \theta_1 - \theta_3 = \delta_1, \quad \theta_2 - \theta_4 = \delta_2$$

hold.

In the case of symmetry ($\beta_1 = \beta_2$), it is obvious that $\theta_1 = \theta_2$ and $\delta_1 = \delta_2 = 0$.

The flow region is broken down into a number of zones (see Fig. 1) in each of which the flow (uniform in an idealized formulation) has its own characteristics. Zone 0, the region of the undisturbed flow, is bounded on the left by any boundary placed in the region of a free supersonic stream (e.g., by a straight line connecting the vertices of the wedges) and on the right — by the fronts of CSs i_1 and i_2 (and additionally by the front of the CS m for MR). Zone 1, the region of the flow developed (clockwise) on the CS i_1 along the surface of the upper wedge, is bounded by the fronts of the CSs i_1 and r_1, respectively, on the left and on the right. Likewise, zone 2, the region of the flow developed (counterclockwise) on the CS i_2 along the surface of the lower wedge, is bounded by the fronts of the CSs i_2 and r_2 on the left and on the right, respectively. Zone 3, the sector of the flow developed (counterclockwise) on the CS r_1, is bounded by its front and the surface of contact discontinuity, which is the boundary of the wake S (for MR — S_1). Zone 4, the sector of the flow developed (clockwise) on the CS r_2, is bounded by its front and the surface of contact discontinuity, which is also the boundary of the wake S (for MR — S_2). In the case of RR, zones 3 and 4 have a common boundary (they close directly), and in the case of MR, zones 5 and 6, the flow regions after the CS m front, are located between them.

Conversions between these two types of reflection are determined by the separation criterion and the Neumann criterion. Both these criteria (bifurcation points) demarcate three regions in which the existence of only MR, MR and RR, and only RR is possible. The process of conversion between these types of reflection in varying the parameters determining the physics of the problem, e.g., the flight velocities and altitudes, can be accompanied by the phenomenon of hysteresis.

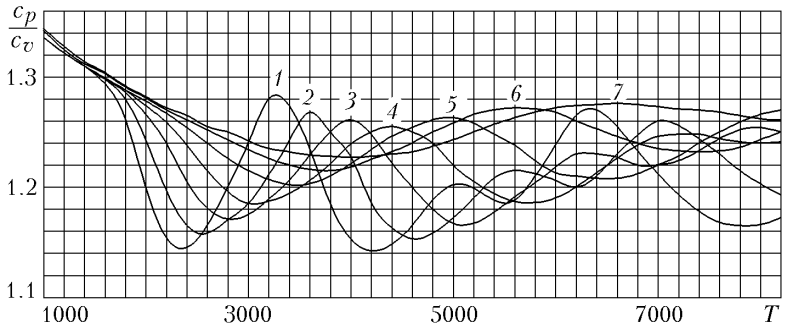

Fig. 2. Temperature dependence of the c_p/c_v ratio (for air) at a varied pressure: 10^{-3} (1), 10^{-2} (2), 10^{-1} (3), 1 (4), 10 (5), 10^2 (6), and 10^3 atm (7).

Studies of the wave structure of these two types (RR and MR) are usually made on the assumption that the physical properties of the gas flow in passing through the whole system of SWs remain unchanged, i.e., the model of an ideal polytropic gas with a constant value of the adiabatic exponent (polytrope) γ throughout the flow region is used (see, e.g., [2]). However, real processes (see [3, 4]), whose investigation is associated with the intensification of the development of hypersonic aircraft, call for the extension of this physical model. Since the problem schematically represented in Fig. 1 models the flow at the entrance to the engine air intake, the level of knowledge about the regimes of this flow, the prediction of interconversions between RR and MR, as well as the answer to the question which of these two types of shock-wave structures is realized in the nonuniqueness domain of the solution and which factors influence this are of great importance in developing a system for controlling the regime of fuel combustion for stable functioning of the propulsion unit on the whole.

In the present paper, to investigate the gas- and thermodynamics of the physical processes [3, 4], the effective adiabatic exponent method (see [5–7]) is used. This method permits simulating a gas flow with regard for its real properties by varying the adiabatic exponent $\gamma(p, T)$, which changes throughout the flow field depending on the local values of pressure p and temperature T.

An illustration of the conclusion that it is necessary to take into account the changes in the thermodynamic properties of the gas in hypersonic streams with zones of high p and T is Fig. 2, which shows the temperature dependence of the heat ratio c_p/c_v for air (classical adiabatic exponent $\gamma = c_p/c_v$) in parametric form, where the parameter is pressure with fixed values for each curve. The data were taken from the tables of [8, 9]. The "wavy" behavior of the curves is due to such physical processes proceeding sequentially with increasing T as excitation of vibrational degrees of freedom of oxygen molecules and their dissociation, excitation of vibrations in nitrogen molecules and their dissociation, and excitation of electron shells of atoms and their ionization.

In the present work, to take into account the real properties of the gas, a physicomathematical model of an SW with various adiabatic exponents before and after the shock front, which is assumed to be an infinitely thin discontinuity, is used. The basic gas- and thermodynamic relations on a discontinuity and an analysis of the range of applicability of the model and its comparison to the model of invariability of the properties of the gas medium in passing through a CS are given in [10].

Methodology of Investigation. To analyze the wave structures arising from the interaction of incident SWs i_1 and i_2 determining the formation of reflected SWs r_1 and r_2 of different types (RR and MR), it is very convenient to use the shock polar technique (see also [11]). This technique permits replacing the complicated mathematical analysis of the results of the simultaneous solution of several, according to the number of interacting SWs, nonlinear algebraic equations relating the parameter values before and after the front of each CS (with the necessity of selecting solutions as a consequence of their nonuniqueness) by a graphic method of obtaining a solution. This method makes the very process of obtaining solutions and their analysis clearer and more logical, and the choice of the required solution in the case of their nonuniqueness presents much smaller difficulties.

By the shock wave polar, or simply the shock polar, is meant the relation relating the flow angularity θ and the pressure ratio $\xi = p_+/p_-$, where p_+ is the pressure after the CS front and p_- before it at a parametric dependence on the Mach number M_- and effective adiabatic exponents γ_+ and γ_-:

$$f(\theta, \xi, M_-, \gamma_-, \gamma_+) = 0 . \quad (1)$$

The graphic curve illustrating dependence (1) strictly called the shock polar (SP) in the plane $(x, y) = (\theta, \xi)$ is a closed curve bounded by values of $\theta_{min} \le \theta \le \theta_{max}$ and $\xi_{min} \le \xi \le \xi_{max}$ and mirror-symmetric about the straight line $\theta_s = 0.5(\theta_{min} + \theta_{max})$. A concrete form of (1) is given in [10, 11], where a detailed analysis of the SP with varied γ_+, γ_-, and M_- has been performed.

In the classical model of invariability of the gas properties, the shock-wave structures of the problem under consideration (Fig. 1) are determined by the following list of parameters:

$$F = (\beta_1, \beta_2, M_0, \gamma) . \quad (2)$$

However, for high-speed gas flows it is necessary to use a physically more real model taking into account the change in the properties of the gaseous medium during passage of the flow through the CS fronts. In this case, the list of parameters (2) is extended:

$$F = (\beta_1, \beta_2, M_0, \gamma_0, \gamma_1, \gamma_2, \gamma_3, \gamma_4) , \quad (3)$$

where γ_i ($i \in [0, 4]$) represents the adiabatic exponents in different flow zones demarcated by the CS fronts (see Fig. 1).

Note that the polars relating the values of γ before and after the passage of the flow through an SW represent two situations: a decrease or an increase in γ. The first situation, from the point of view of the physics of the process, is realized more frequently: after a shock additional degrees of freedom (e.g., vibrational ones) of the gas molecules are excited and the value of γ decreases (decreasing portions of the curves in Fig. 2). The second situation represents the domain of parameters before and after the shock front situated on the increasing portions of the curves in Fig. 2, e.g., in the 2400–3300 K temperature range for a pressure of 10^{-3} atm or in the 3100–4200 K range for a pressure of 1 atm. On these portions, not the process of excitation of the degrees of freedom of molecules but their dissociation causing an increase in γ is dominant. A detailed description of the model of the effective adiabatic exponent, the range of its applicability, the gas-dynamic relation, and its distinction from the classical model are given in [6, 7, 10], and the influence of γ_i on the form of the SP has been investigated in [11].

In applied aerodynamic problems on the motion of an arbitrary object in the Earth's atmosphere (in the present paper, this is a problem on the flow in the HRE air intake), as a rule, the following basic parameters are given: entrance geometry (angles β_1 and β_2 in Fig. 1) and flight altitude H and velocity V. In so doing, neither the Mach number M_0 nor the values of the effective adiabatic exponent not only in the region of the undisturbed flow but also in the zone of the incoming undisturbed flow determining the whole shock-wave pattern are known directly. In some aspect, this is a positive factor, since the list of diagnostic variables (3) is not only considerably shorter:

$$F = (\beta_1, \beta_2, H, V) , \quad (4)$$

but its components have a more "transparent" meaning excluding an indefinite interpretation — geometric flow angularities and flight altitude and velocity of the hypersonic aircraft. Variation of the values of parameters (4) may lead to the formation of different types of shock-wave structures. It is very convenient for analysis to select from the list of parameters (4) one parameter, e.g., β_2, which is declared as a "reference" for analysis. In the space of allowable values of β_2, there exist two special points:

$$\beta_2^* = \beta_2^*(\beta_1, H, V) , \quad \beta_2^{**} = \beta_2^{**}(\beta_1, H, V) . \quad (5)$$

They are called, respectively, the lower and upper (since $\beta_2^* < \beta_2^{**}$) bifurcation points of the solution and define the following ranges of shock-wave structures:

$$\beta_2 < \beta_2^* , \quad \text{only RR is possible ;}$$

$$\beta_2^* \le \beta_2 \le \beta_2^{**} , \quad \text{both RR and MR are possible ;} \quad (6)$$

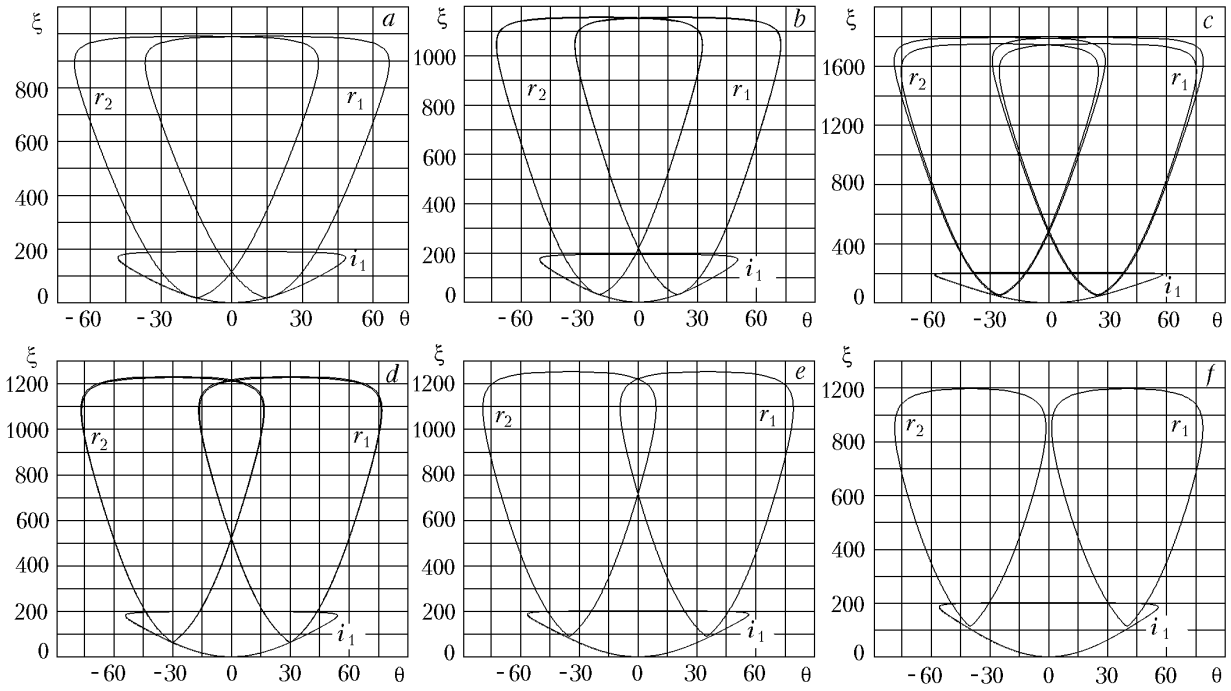

Fig. 3. Polars of the incident shock wave i_1 and two reflected shock waves r_1 and r_2 at fixed values of H = 40 km and V = 4 km/sec and varied wedge angles $\beta_1 = \beta_2 = 15^o$ (a), 20^o (b), 25^o (c), 30^o (d), 35^o (e), and 40^o (f).

$$\beta_2 > \beta_2^{**}, \quad \text{only MR is possible .}$$

Even without knowing the numerical values of β_2^* and β_2^{**}, it is possible to determine by the graphs of shock polars (see Fig. 3) which of the shock-wave structures (6) is realized at a certain set of parameters (4). Let us write these conditions analogous to (6) in the same sequence but in a different formulation:

$$\begin{gathered} 1)\ \text{if } r_1 \text{ and } r_2 \text{ polars intersect inside } i_1 \text{ polar, then MR is impossible ;} \\ 2)\ \text{if } r_1 \text{ and } r_2 \text{ polars intersect outside } i_1 \text{ polar, then both RR and MR are possible ;} \\ 3)\ \text{if } r_1 \text{ and } r_2 \text{ polars do not intersect, then RR is impossible .} \end{gathered} \tag{7}$$

Generally speaking, not only for β_2 but also for each of the other parameters of (4) can the notion of the lower and upper bifurcation points be introduced: $\beta_1^*(\beta_2, H, V)$ and $\beta_1^{**}(\beta_2, H, V)$, $H^*(\beta_1, \beta_2, V)$ and $H^{**}(\beta_1, \beta_2, V)$, $V^*(\beta_1, \beta_2, H)$ and $H^{**}(\beta_1, \beta_2, H)$. In the general form, bifurcation points are some three-dimensional hypersurfaces in the four-dimensional space (4):

$$f^*(\beta_1, \beta_2, H, V) = 0\ , \quad f^{**}(\beta_1, \beta_2, H, V) = 0\ . \tag{8}$$

Naturally, the forms of writing (5) and (8) are equivalent and for each specific problem their most suitable form can be used.

Note that apart from determining the boundaries of regimes the shock-polar technique permits obtaining numerical characteristics of the flows (Fig. 1): the relative and absolute values of the pressure and the flow angularity at the fronts of all CSs and by them the values of all the other gas-dynamic parameters and slope angles of the shock waves throughout the flow region are determined. Consider sequentially the influence of the basic parameters (entrance

TABLE 1. Flow Parameters at H = 40 km, V = 4 km/sec and Varied Values of $\beta_1 = \beta_2 = \beta$

β	Parameters	Zones				
		0	1	3	2	4
15^o	γ	1.40	1.33	1.31	1.33	1.31
	M	12.61	6.57	7.77	6.57	7.77
	p	0.00283	0.0548	0.0548	0.0548	0.0548
	T	250	1145	1325	1145	1325
30^o	γ	1.40	1.23	1.23	1.23	1.23
	M	12.61	4.18	3.44	4.18	3.44
	p	0.00283	0.181	0.567	0.181	0.567
	T	250	3600	4600	3600	4600
40^o	γ	1.40	1.20	1.22	1.20	1.22
	M	12.61	3.01	2.51	3.01	2.51
	p	0.00283	0.295	0.572	0.295	0.572
	T	250	5840	6390	5840	6390

angle, flight altitude and velocity) on the gas-dynamics of the flow in the diffuser, taking into account the real physical properties of the air medium in a wide range of change in the temperatures and pressure.

Symmetric Flow. Figure 3 shows the results of the numerical simulation (the computational algorithm is described in detail in [11]) of the problem at fixed values of the flight altitude H = 40 km and velocity V = 4 km/sec in the Earth's atmosphere. The angles of entrance to the HRE air intake were assumed to be equal ($\beta_1 = \beta_2 = \beta$) and had values of 15, 20, 25, 30, 35, and 40^o. According to (7), it may be concluded at once that at $\beta = 15^o$ only the regular and at $\beta = 40^o$ only the Mach shock-wave structure of the flow is possible. In the other variants given, both types of shock-wave structures are possible. At such H and V the values of the lower and upper bifurcation points (5) are approximately equal to $\beta^* \approx 19.9^o$ and $\beta^{**} \approx 39.8^o$, respectively. In the domain of solution dualism, the r_1 and r_2 polars "split" into Mach r_{1M}, r_{2M} and regular r_{1R} and r_{2R} polars (not marked in the figure). The degree of their splitting and the order of embedment in one another depend on which portion (see Fig. 2) of the $\gamma(p, T)$ curve — increasing or decreasing — the shock-wave transition occurs (for details, see [11]). Note that the question of solution selection requires a special study and is beyond the scope of the present work.

The most important parameters in different flow zones — the adiabatic exponent γ, the local Mach number M, the pressure p, and the temperature T for angles β = 15, 30, and 40^o — are given in Table 1 and correspond to the variants shown in Fig. 3a, d, f. The sequence of zones in the tables is given for the convenience of comparing the nearby numbers. The shock of parameters on the incident shock wave i_1 is a jump from the values in zone 0 to the values in zone 1; the shock on reflected SWs is a jump from the values in zone 1 to the values in zone 3 (for r_1) and from the values in zone 2 to the values in zone 4 (for r_2). In the case of a symmetric problem, the numbers in columns 1 and 2, 3 and 4 coincide; these values were saved for unification of information presented in the other tables for asymmetric problems.

Notice the following features. On the shock i_1 there is a marked change in the properties of the gaseous medium: the adiabatic exponent γ changes from 1.40 to 1.33 (for $\beta = 15^o$), 1.23 (for $\beta = 30^o$), and 1.20 (for $\beta = 40^o$). The decrease in γ is due to the significant increase in the excitation of vibrational degrees of freedom in the oxygen O_2 molecules at $\beta = 15^o$ and even in the nitrogen N_2 molecules at $\beta = 40^o$, when considerable values of temperatures are reached, about 5840 K at a pressure of 0.3 atm (the statistical pressure in the incoming flow at this altitude is 0.0028 atm). The passage of the stream through the reflected, less intensive shock r_1 changes the properties of the gaseous medium to a lesser extent, and differently, depending on β. At $\beta = 15^o$ the adiabatic exponent decreases, as on i_1, but insignificantly (excitation of O_2 molecules is going on), from 1.33 to 1.31. At $\beta = 30^o$ γ retains its value of 1.23, and at $\beta = 40^o$ there is an increase in γ from 1.20 to 1.22, which is now due to the process of N_2 molecule dissociation rather than vibration excitation.

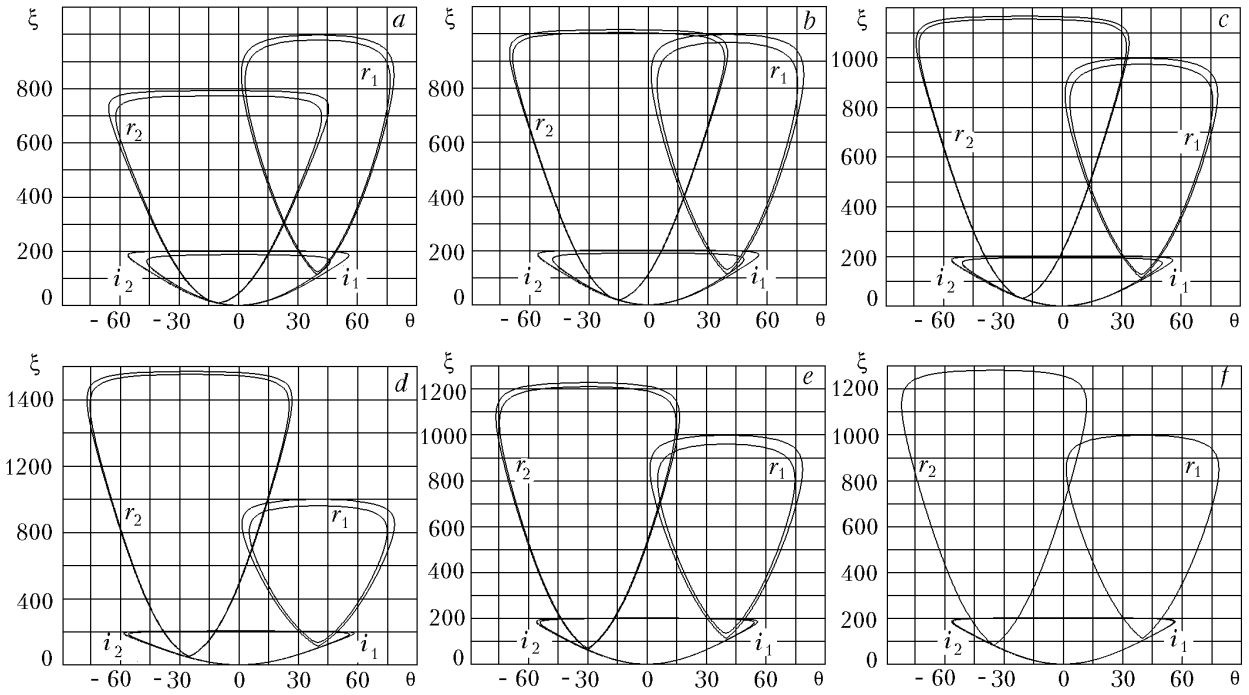

Fig. 4. Polars of two incident shock waves i_1 and i_2 and two reflected shock waves r_1 and r_2 at fixed values of H = 40 km and V = 4 km/sec, $\beta_1 = 40^o$ and varied values of $\beta_2 = 10^o$ (a), 15^o (b), 20^o (c), 25^o (d), 30^o (e), and 35^o (f).

Notice also the fact associated with the solution nonuniqueness at $\beta = 30^o$. In Table 1, in zone 3 (and 4) values corresponding to the Mach reflection are given. At regular reflection the following values reach the steady state: γ = 1.22, M = 2.44, p = 1.47, and T = 6530, which differ considerably, except for γ, from the "Mach" values.

In visual analysis, the difference between the MR and RR parameters is determined by the "remoteness" of the polar intersection points $(i_1 \times r_1)$ and $(i_1 \times r_2)$. In particular, at $\beta_2 = \beta_2^*$ (Fig. 3b) these parameters coincide, and at $\beta_2 = \beta_2^{**}$ (Fig. 3f) the difference is maximum. Thus, the question on exactly what solution — Mach or regular — becomes stationary in the nonuniqueness domain is of great importance for the HRE functioning.

Asymmetric Flow. *Wide angle* β_1. Consider the influence on the flow structure of the angle β_2 variation with all other parameters of list (4) being fixed: H = 40 km, V = km/sec, $\beta_1 = 40^o$. The systems of polars corresponding to the values of β_2 = 10, 15, 20, 25, 30, and 35^o are given in Fig. 4. The choice of β_1 and β_2 values is due to the following facts. The angle of 40^o is close to the limit angle at which a compression shock attached to the vertex of a wedge can exist and the formation of shock-wave structures shown in Fig. 1 is possible.

The small angle of 10^o always provides the regular type of reflection. Thus, practically all interesting structures of the flow are formed by angles lying in this range. This permits, in analyzing the shock polars (see Fig. 4), approximate determination of the flow structure at other values of β_1 and β_2, "moving mentally" the r_1 and r_2 polars to the reference points of the polar i_1 corresponding to these values. It is clear that such a visual approximation will not ensure the obtaining of "exact" numbers but can give quickly, without numerical calculation, a general useful idea about the change in the shock-wave structure of the flow at varied β_1 and β_2.

Notice the splitting of incident SW polars i_1 and i_2 due to the fact that $\beta_1 \neq \beta_2$. The polar swing depends on the value of γ after the incident CS front: the smaller this value, the larger the width and height of the polar (a detailed study was made in [10, 11]). This value is determined by the whole list (4). In our case, the i_2 polar is "embedded" in the i_1 polar at all values of β_2 (see the values of γ in Table 2). The nature of the splitting of the r_1 and r_2 polars is described above.

Analyzing Fig. 4, it may be concluded that at the given values of β_1, H, and V throughout the range of variation of β_2 the domain of solution nonuniqueness takes place: both MR and RR are possible. In the practice of HRE development this makes such a part of the parameter field very unpleasant in developing control systems, since exact

TABLE 2. Flow Parameters at H = 40 km, V = 4 km/sec, $\beta_1 = 40^o$ and Varied β_2

β_2	Parameters	Zones				
		0	1	3	2	4
10^o	γ	1.40	1.20	1.22	1.37	1.19
	M	12.6	3.01	2.51	7.99	5.03
	p	0.00283	0.295	0.572	0.0281	0.532
	T	250	5830	6390	682	3290
20^o	γ	1.40	1.20	1.22	1.29	1.21
	M	12.6	3.01	2.51	5.58	4.64
	p	0.00283	0.295	0.572	0.0899	0.553
	T	250	5830	6390	1800	3460
30^o	γ	1.40	1.20	1.22	1.23	1.23
	M	12.6	3.01	2.51	4.18	3.44
	p	0.00283	0.295	0.572	0.181	0.567
	T	250	5830	6390	3600	4600

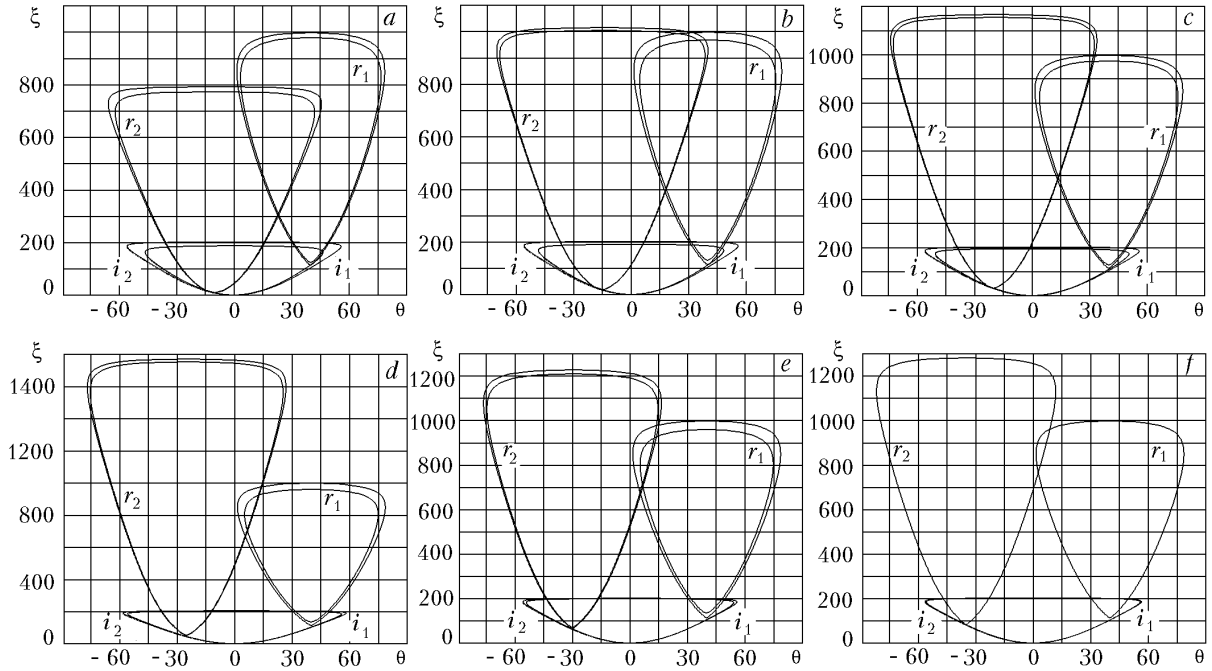

Fig. 5. Polars of two incident shock waves i_1 and i_2 and two reflected waves r_1 and r_2 at fixed values of H = 40 km and V = 4 km/sec, $\beta_1 = 15^o$ and varied values of $\beta_2 = 20^o$ (a), 25^o (b), 30^o (c), 35^o (d), 40^o (e), and 45^o (f).

prediction of which of the regimes will be realized seems to be unjustifiably optimistic because of the influence on this process of a large number of factors, in particular, the previous history of the flow (for more details, see [13, 14]). The boundaries of the solution dualism domain can be roughly estimated on the basis of visual analysis. Taking, for example, Fig. 4b and "moving mentally" the r_1 polar to the left (so that the central point of r_1 always rests on the i_1 polar) and simultaneously extending it, which corresponds to a decrease in β_1, we will follow the "movement" of the intersection point of r_1 and r_2. The moment this point "enters" the i polar (intersection point of three polars i_1, r_1, and r_2 at a time) is the boundary of the domain of existence of the Mach type of reflection. This is the lower bifurcation point of the solution $\beta_1^*(\approx 18^o)$. Then, at $\beta_1 < \beta_1^*$ the existence of only one type of SW-structure — regular reflection — is possible.

TABLE 3. Flow Parameters at H = 40 km, V = 4 km/sec, $\beta_1 = 15^o$ and Varied β_2

β_2	Parameters	Zones				
		0	1	3	2	4
20^o	γ	1.40	1.33	1.18	1.29	1.19
	M	12.6	6.57	5.77	5.58	5.17
	p	0.00283	0.0548	0.446	0.0899	0.446
	T	250	1150	2910	1800	3230
25^o	γ	1.40	1.33	1.19	1.17	1.21
	M	12.6	6.57	5.20	6.10	4.45
	p	0.00283	0.0548	0.542	0.127	0.582
	T	250	1150	3210	2800	3550
30^o	γ	1.40	1.33	1.19	1.23	1.23
	M	12.6	6.57	5.20	4.18	3.44
	p	0.00283	0.0548	0.542	0.181	0.567
	T	250	1150	3210	3600	4600

Likewise, by visual analysis, with a low degree of accuracy, of course, we can also determine the upper bifurcation point β_1^{**}. For example, from Fig. 4b it is seen that this point at a fixed value of $\beta_2 = 15^o$ cannot exist because the motion of the r_i polar on the i_1 polar to the right is limited by the value of $\theta_{max} \approx 55^o$. In this case, the intersection point of the r_1 and r_2 polars will always exist, i.e., the possibility of RR will always remain together with the possibility of existence of MR. RR can only be forbidden by increasing β_2, i.e., only by shifting the r_2 polar to the left.

Some of the numerical results of computer simulation of this type of problem are presented in Table 2 for β_2 = 10, 20, and 30^o. The structure of the table was described in the previous section. Note that the question of legitimacy of using the model of a continuum (accuracy of results obtained) at large altitudes is rather debatable, but, in any case, these data are very useful, in particular, for analyzing the dynamics of change in the SW-structure and gasdynamic parameters in various flow zones at varied flight altitudes. Moreover, in [12] the comparison of the data obtained as a result of numerical experiments in solving the Euler (Navier–Stokes) and Boltzmann equations showed a good correlation up to the values of $H \approx 120$ km.

Let us analyze the numerical values given in Table 2. Here the variant of $\beta_2 < \beta_1$ is presented (Table 3 gives data, on the contrary, for $\beta_2 > \beta_1$). Since β_1 = const in this case, the values in columns 1 and 3 (and especially in column 0) are equal for one and the same type of reflection (MR and RR), but for unification of the representation of the results the structure of the tables is not changed because of this, since at a general variation of the parameters of list (4) in all positions of the table the numbers are substantially different.

The adiabatic exponent γ, which is equal to 1.40 in the undisturbed flow zone, reflects, on the average, the physicochemical processes proceeding as the gas passes through the compression shocks (excitation of vibrations of atoms in molecules, their dissociation and ionization at high temperatures). On incident CSs i_1 and i_2 the value of γ decreases.

For instance, in zone 1 γ_1 = 1.20, and in zone 2, naturally, it depends on the varied value of β_2: at β_2 = 10, 20, and 30^o γ_2 = 1.37, 1.29, and 1.23, respectively, which reflects the intensification of the vibrational process in the O_2 molecules. On reflected CSs r_1 and r_2 as less intense compared to the incident ones, γ changes to a lesser extent, i.e., the change in the properties of the gaseous medium is smaller.

At the exit from the system of shocks the flow becomes very nonuniform, especially at a wide difference between β_1 and β_2. For instance, at $\beta_2 = 10^o$ in the adjacent zones 3 and 4 the following values of temperatures are attained: T_3 = 6390 K and T_4 = 3290 K. The pressures differ less noticeably: p_3 = 0.572 atm and p_4 = 0.532 atm. Note that these data are given for the MR type. If the RR type is realized, then considerably larger values of these quantities will take place: T_3 = 6860 K and T_4 = 4590 K at $p_3 = p_4$ = 0.879 atm. It will be recalled that at RR the pressures in zones 3 and 4 are always the same and these zones are separated by a tangential discontinuity, and at MR between zones 3 and 4 metastable zones 5 and 6 of the flow after the central shock m are situated (see Fig. 1b).

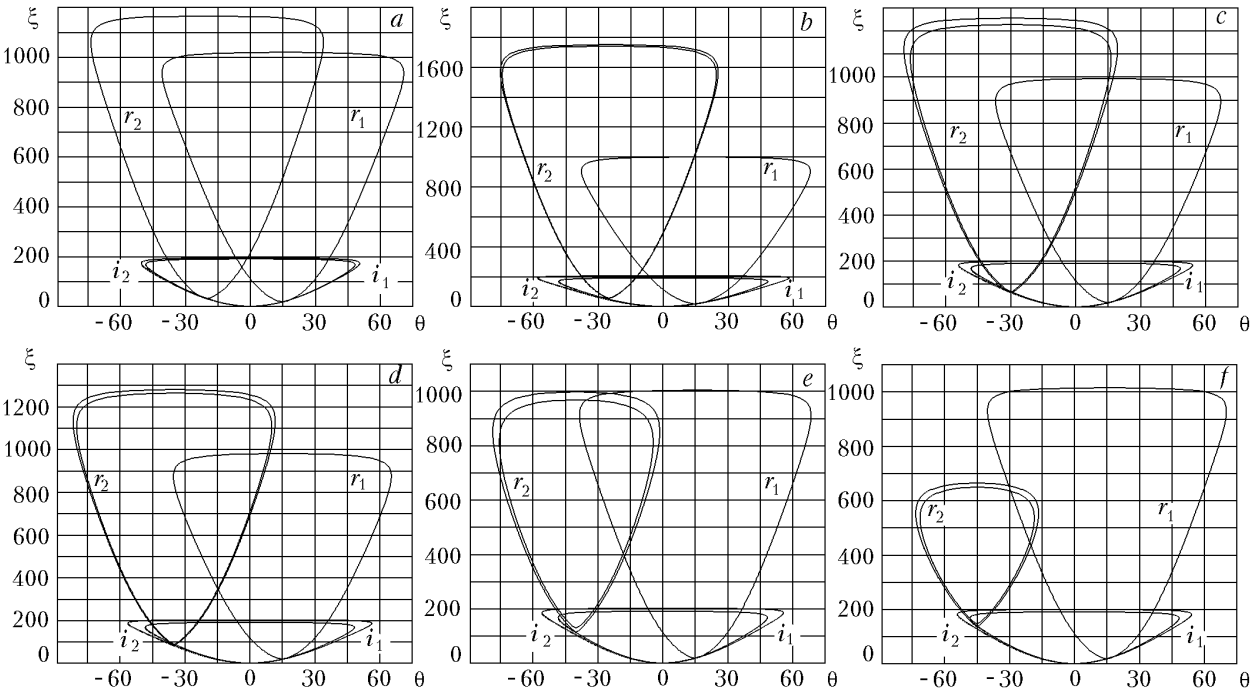

Fig. 5. Polars of two incident shock waves i_1 and i_2 and two reflected waves r_1 and r_2 at fixed values of H = 40 km and V = 4 km/sec, $\beta_1 = 15^o$ and varied values of $\beta_2 = 20^o$ (a), 25^o (b), 30^o (c), 35^o (d), 40^o (e), and 45^o (f).

Thus, to optimize the form of entrance to the diffuser by a number of indices (maximum of the statistical pressure or flow at the exit), it is necessary first to answer the fundamental question which type of shock-wave structure is realized. The elaborated special computational algorithm for determining the bifurcation points in the parametric space (4) has demonstrated a high efficiency of functioning in a wide range of diagnostic variables. It should be noted, however, that the process of search for extrema in a four-dimensional space with their nonmonotonic dependence on some of the "coordinates" of (4) requires much computer time. Calculations can be promoted by organizing a parallel count on multiprocessor systems (for parallelizing of solutions of gas-dynamics problems, see [15, 16]).

Small angle β_1. We now turn to the analysis of the influence on the flow structure of the variation of β_2 at a fixed flight altitude H = 40 km and velocity V = 4 km/sec with a small value of $\beta_1 = 15^o$. The systems of polars corresponding to the values of β_2 = 20, 25, 30, 35, 40, and 45^o are given in Fig. 5. The reasons for choosing these angles are the same as in the previous section. Only note that the results for small $\beta = 0.5^o$ and so on are not analyzed here, since the central counterpoint of this work is the investigation of the range of nonuniqueness of solutions.

The polar patterns are analogous, in general, to those considered earlier. There are two split polars of i_1 and i_2 shocks incident inside the region from wedge angles β_1 and β_2. For these parameters, the i_1 polar is embedded in i_2.

The polars of reflected shocks r_1 and r_2 also split into a Mach one and a regular one. This occurs in the case of dualism of solutions, where the existence of both MR and RR is possible, which takes place almost throughout the range of the investigated β_2, except for the variant with $\beta_2 = 20^o$, where MR is impossible. Note that the splitting of r_1 polars is practically visually imperceptible (and can only be analyzed by numerical data), and the splitting of r_2 polars is maximum at $\beta_2 = 45^o$ (Fig. 5f).

Table 3 gives some of the numerical data for flows with β_2 = 20, 25, and 30^o corresponding to Fig. 5a, c, e. The i_1 and i_2 CSs incident inside the flow have a substantially different effect on the gaseous medium. The adiabatic exponent varies from the value of 1.40 in the incoming flow for angles β_2 = 20, 25, and 30^o on the i_1 CS (in zone 1), respectively, to equal values of "only" 1.33, and on the i_2 CS (in zone 2) to the values of 1.29, 1.17, and 1.23. Notice the value of γ = 1.17. While the very fact that the shock action on the medium of the shock attached to the wedge β_2 leads to a greater change in γ than the action of the shock from the wedge $\beta_2 = 15^o$ is rather expected, since the intensity of the i_1 CS is lower than that of the i_2 CS, the numerical result γ = 1.17 is absolutely unpre-

dictable (nonmonotonic in β_2 and too drastic a change in the properties of the medium). In so doing, the temperature increases in the i_1 CS (in zone 1) from the value in the incoming flow T_0 = 250 K to T_1 = 1150 K and in the i_2 CS (in zone 2) to T_2 = 1800 K (for $\beta_2 = 20^o$), T_2 = 2800 K (for $\beta_2 = 25^o$), and T_2 = 3600 K (for $\beta_2 = 30^o$). In the region of temperatures $T \approx 2800$ K, intensive excitation of vibrations in the O_2 molecules occurs, and in the region of temperatures $T \approx 3600$ K the oxygen is almost completely dissociated and the deviation of γ from its value for the diatomic gas of 7/5 provides only a vibration excitation of the nitrogen N_2 molecules.

After the passage of the system of r_1 and r_2 CSs in zones 3 and 4 the temperatures have the values of T_3 = 3210 K (3810 K) and T_4 = 4600 K (5280 K) for the variant with $\beta_2 = 30^o$. Here the values for both the Mach and regular (bracketed) types of reflection are given.

A much higher inhomogeneity of the flow temperature at the outlet takes place for a large angle (not given in Table 3) with a value of $\beta_2 = 45^o$ (here the existence of both MR and RR is also possible): T_3 = 3210 K (5790 K) and T_4 = 6900 (8750 K). There is also a considerable difference between the adiabatic exponents: γ_3 = 1.19 (1.19), γ_4 = 1.24 (1.25) and the local Mach numbers: M_3 = 5.20 (3.26) and M_4 = 1.89 (1.17). It will be recalled that the Mach number of the incoming flow M_0 = 12.6. Note that the pressure in these zones does not differ very much: p_3 = 0.542 atm (1.27 atm) and p_4 = 0.563 atm (1.27 atm).

On the whole, the graphs of the shock polars and the numerical data in the tables complementing them provide very interesting information about the shock-wave structures and values of the gas-dynamic parameters in different flow zones.

CONCLUSIONS

Direct numerical simulation of flows on the basis, in particular, of Euler equations in the domain of solution nonuniqueness poses its own, specific problems. Since the computational algorithm can obtain only one specific solution, the following questions arise: what solution is this (MR or RR) and what factors influence the obtaining of exactly this solution. For example, what are the basins of attraction of the solution: when various input data are used, if establishment methods are used; when other algorithmic parameters — dimensions and configurations of the calculation mesh, etc. are varied. The question on the character of the computational process in the vicinity of the bifurcation points of the solution is interesting: are there spontaneous transitions from one branch of the solution to the other, especially in attempting to obtain in the end one type of solution, starting from the other type? Or does the algorithm "determine independently" only one type of solution, completely ignoring the other type?

Let us emphasize that the main "danger" of direct numerical simulation of complex problems of gas dynamics in an area that has been little studied or not studied at all, where there is no support by either analytical relations or experimental data serving as a certain reference point, is the probability of obtaining some "proper" solution (such questions are described in detail in [14, 17]). This especially holds for the recently developed large number of algorithms of the so-called "increased" order of accuracy and their application for calculating problems with a complicated shock-wave configuration. For example, in [18, 19] it has been shown that all algorithms used yielded different (some of them radically different) solutions to one and the same problem.

Therefore, theoretical studies revealing special domains of behavior of solutions are becoming again a very important element in the advancement of numerical simulation to the region of hypersonic real gas flows.

This work was supported by the Russian Basic Research Foundation (project No. 02-01-00097).

NOTATION

c_p, heat capacity at a constant pressure; c_v, heat capacity at a constant volume; H, flight altitude, km; i, incident shock; m, central shock; M, Mach number; p, pressure, atm; r, reflected shock; S, wake; T, temperature, K; V, flight velocity, km/sec; β, wedge angle; γ, adiabatic exponent; δ, wake angle; φ, shock slope; ξ, pressure ratio after and before a shock; θ, flow angularity. Subscripts: 0, 1, 2, 3, 4, flow zone numbers; + (plus), parameters after the shock front; − (minus), parameters before the shock front; min, minimum value; max, maximum value; s, mean value.

REFERENCES

1. T. A. Bormotova, V. V. Volodin, V. V. Golub, and I. N. Laskin, Thermal correction of the inlet diffuser of a hypersonic ramjet engine, *Teplofiz. Vys. Temp.*, **41**, No. 3, 472–475 (2003).
2. H. Li and G. Ben-Dor, Analytical and experimental investigations of the reflection of asymmetric shock waves in steady flows, *J. Fluid Mech.*, **390**, 25–43 (1999).
3. Ya. B. Zel'dovich and Yu. P. Raizer, *Physics of Shock Waves and High-Temperature Hydrodynamic Phenomena* [in Russian], Nauka, Moscow (1966).
4. J. F. Clarke and M. McChesney, *The Dynamics of Real Gases* [Russian translation], Mir, Moscow (1967).
5. I. Prigogine and D. Kondepudi, *Modern Thermodynamics. From Thermal Engines to Dissipative Structures* [Russian translation], Mir, Moscow (2002).
6. G. A. Tarnavsky and S. I. Shpak, Effective specific heat ratio for problems of real gas hypersonic flows at bodies, *Thermophys. Aeromech.*, **8**, No. 1, 39–53 (2001).
7. G. A. Tarnavskii and S. I. Shpak, Methods of calculation of an effective adiabatic index in computer simulation of hypersonic flows, *Sib. Zh. Industr. Mat.*, **4**, No. 1(7), 177–197 (2001).
8. *Tables of Thermal Properties of Gases*, USA, New York Nat. Bureau of Standards, Circular 564 (1955).
9. N. B. Vargaftik, *Handbook on Thermophysical Properties of Gases and Liquids* [in Russian], Fizmatgiz, Moscow (1963).
10. G. A. Tarnavskii, Shock waves in gases with different adiabatic indices before and after the shock front, *Vych. Met. Program.*, **3**, No. 2, 129–143 (2002).
11. G. A. Tarnavskii, Nonuniqueness of shock-wave structures in real gases: Mach and/or regular reflection, *Vych. Met. Program.*, **4**, No. 2, 258–277 (2003).
12. V. M. Kovenya, G. A. Tarnavskii, and S. G. Chernyi, *Use of the Splitting Method in Aerodynamics Problems* [in Russian], Nauka, Novosibirsk (1990).
13. G. A. Tarnavskii and S. I. Shpak, Some aspects of computer simulation of hypersonic flows: Stability, nonuniqueness and bifurcation of numerical solutions of the Navier–Stokes equations, *Inzh.-Fiz. Zh.*, **74**, No. 3, 125–132 (2001).
14. G. A. Tarnavskii, G. S. Khakimzyanov, and A. G. Tarnavskii, Modeling of hypersonic flows: Effect of starting conditions on the final solution in the vicinity of bifurcation points, *Inzh.-Fiz. Zh.*, **76**, No. 5, 54–60 (2003).
15. G. A. Tarnavskii and S. I. Shpak, Decomposition of the methods and parallelizing of algorithms of solution of aerodynamics and physical gas dynamics problems, *Programmirovanie*, No. 6, 45–57 (2000).
16. G. A. Tarnavskii, V. D. Korneev, D. A. Vainer, N. M. Pokryshkina, A. Yu. Slyunyaev, A. V. Tanaseichuk, and A. G. Tarnavskii, Computation system "Potok-3": Experience of parallelizing the computation complex. Pt. 1. Ideology of parallelizing, *Vych. Met. Program.*, **4**, No. 1, 37–48 (2003).
17. V. F. Volkov, and G. A. Tarnavskii, Symmetry breaking and hysteresis of stationary and quasistationary solutions of the Euler and Navier–Stokes equations, *Zh. Vych. Mat. Mat. Fiz.*, **41**, No. 11, 1742–1750 (2001).
18. M. Pandolfi and D. D'Ambrosio, Numerical instabilities in upwind methods: Analysis and cures for the "carbuncle" phenomena, *J. Comput. Phys.*, **166**, No. 2, 271–301 (2001).
19. J. Shi, Y.-T. Zhang, and C.-W. Shu, Resolution of high order WENO schemes for complicated flow structures, *J. Comput. Phys.*, **186**, No. 2, 690–696 (2003).